Zeolite Characterization and Catalysis

Arthur W. Chester • Eric G. Derouane
Editors

Zeolite Characterization and Catalysis

A Tutorial

Springer

Editors
Arthur W. Chester
Dept. of Chemical and Biochemical Engineering
Rutgers University
Piscataway, NJ 08854
USA
achester@rci.rutgers.edu

Prof. E.G. Derouane
Formerly Departamento de Química
Bioquímica e Farmácia
Faculdade de Ciências e Tecnologia
Universidade do Algarve
8005-139 FARO
Portugal

ISBN 978-1-4020-9677-8 e-ISBN 978-1-4020-9678-5
DOI: 10.1007/978-1-4020-9678-5
Springer Dordrecht Heidelberg London New York

Library of Congress Control Number: 2009937221

*Cover illustration:*Atlas of Zeolite Structures, 5th Ed., Elsevier, 2001

Cover design: WMXDesign GmbH, Heidelberg, Germany

Printed on acid-free paper

Springer is part of Springer Science+Business Media (www.springer.com)

Preface

The idea for putting together a tutorial on zeolites came originally from my co-editor, Eric Derouane, about 5 years ago. I first met Eric in the mid-1980s when he spent 2 years working for Mobil R&D at our then Corporate lab at Princeton, NJ. He was on the senior technical staff with projects in the synthesis and characterization of new materials. At that time, I managed a group at our Paulsboro lab that was responsible for catalyst characterization in support of our catalyst and process development efforts, and also had a substantial group working on new material synthesis. Hence, our interests overlapped considerably and we met regularly. After Eric moved back to Namur (initially), we maintained contact, and in the 1990s, we met a number of times in Europe on projects of joint interest. It was after I retired from ExxonMobil in 2002 that we began to discuss the tutorial concept seriously. Eric had (semi-)retired and lived on the Algarve, the southern coast of Portugal. In January 2003, my wife and I spent 3 weeks outside of Lagos, and I worked parts of most days with Eric on the proposed content of the book.

We decided on a comprehensive approach that ultimately amounted to some 20+ chapters covering all of zeolite chemistry and catalysis and gave it the title *Zeolite Chemistry and Catalysis: An integrated Approach and Tutorial*. Over the next several years, we sought authors for these chapters among both industry and academia. Inclusion of industrial authors was important, since so much of early zeolite science was developed in the industry, before it became a major academic subject. But many industrial authors had difficulty with finding the time and feared that their company proprietary restrictions would hamper them. So many times we had to go back and find new authors.

When Eric suddenly passed away last year (2008), our author list was essentially complete, but we had only six chapters in hand. Other chapters did not appear to be close to completion, and I was afraid that existing material could "age out." The publisher then agreed to a more limited book based on the existing chapters. Review of the existing contents led me to change the title to the more limited *Zeolite Chemistry and Catalysis; A Tutorial*. But late in 2008, with all seven proposed chapters in hand, I realized that the characterization coverage would be much more complete if we had a chapter covering the very important NMR techniques now

utilized broadly. After recommendations from the authors, Dr. Michael Hunger graciously agreed to write such a chapter under a very short deadline (2 months!).

Thus the first five chapters of the book provide tutorials in the major areas of zeolite characterization: X-ray powder diffraction, NMR, temperature programmed desorption and adsorption calorimetry, electron microscopy, and infrared spectroscopy. All these techniques provided major contributions to the development of zeolite science, particularly XRD, IR, and measurement of acid–base properties in the early days (1955–1980). In the 1980s, electron microscopy and NMR started to become more prominent and now are equally important. The only major zeolite characterization area not directly addressed here is electron diffraction, although it was planned in the original contents.

The subsequent chapters deal with theory and catalysis. It has become quite common now with improved theory and high-speed computers to predict zeolite properties and reactivities on strictly theoretical grounds, as outlined in Chap. 6. The two remaining chapters outline the principles and practice of C1 chemistry, a field made possible by zeolites, and the breadth of zeolite catalysis in the chemical industry. What is missing is a description of zeolite catalysis in the refining industry, which drove the initial development of zeolite catalysts, but much of that is actually described in Chap. 8.

The book should be useful in allowing new practitioners, whether students or practicing scientists in other fields, to quickly become familiar with the principles of zeolite science and to apply that understanding to their own fields. Newly developed catalytic materials – ordered mesoporous materials, MOFs (metal-organic frameworks), framework phosphates, and hierarchal nanomaterials – all have their roots in zeolite science, and so an understanding of the basics is important.

The book is dedicated to Eric Derouane and a memoriam is included following the Preface, written by his friends Fernando Ramôa Ribeiro and Jacques C. Védrine.

A Brief Introduction to Zeolites

Zeolites are porous crystalline framework materials containing pores of molecular size (5–12 Å or 0.5–1.2 nm). The term *zeolite* is derived from the Greek words for "boiling stone," from the ability of these materials to absorb water and release it upon heating. Conventional zeolites are based on silicate frameworks in which substitution of some of the Si with Al (or other metals) leads to a negative charge on the framework, with cations (usually Na or other alkaline or alkaline earth metals) within the pore structure. This leads to another important property, ion exchange, where the metal ions in the pore structure can be replaced by other cations (e.g. metal, ammonium, quaternary ammonium).

The zeolitic frameworks are networks composed of tetrahedral T atoms (T=Si, Al, etc.) linked by oxygen ions. Common building blocks of zeolite structures consist of 3, 4, 5, and 6 membered rings (n-MR). Each n-MR consists of n T atoms linked in a ring by O ions and thus actually has $2n$ atoms; thus a 6-MR has 12 total atoms. The structures are arranged such that they form larger rings that represent the molecular pores – commonly 8-, 10- and 12-MR, although structures with 9-, 14-, 18-, and 20-MR pores are known. The 8-, 10-, and 12-MR containing zeolites are

commonly known as *small, intermediate,* and *large* pores. Small pore zeolites will generally allow *n*-paraffins to be adsorbed, while large pore zeolites allow all highly branched paraffins to be absorbed as well. Intermediate pore zeolites are just that, allowing some branched chain but not highly branched paraffins to be adsorbed. Thus zeolites are part of the larger class of materials called *molecular sieves*, which allow mixtures of molecules of differing structures to be separated.

Zeolites occur naturally and are generally formed in alkaline environments from volcanic sediments and materials. The first zeolite discovered and identified as such was stilbite; common abundant zeolites are analcime, clinoptilolite, erionite, heulandite, laumontite, and mordenite. Many of these materials have valuable properties as sorbents and even catalysts, but the natural forms often have faults and irregularities in their structures that limit their application. It is the development of laboratory methods of synthesizing zeolites that led to the many commercial applications of zeolites.

The first synthetic zeolite was made from Na, Si, and Al at Linde's laboratories in Tonawanda, NY. It was termed *zeolite A*, being the first, and was found to be composed of sodalite cages arranged to give 8-MR pores. Zeolite A was capable of adsorbing water and *n*-paraffins as well. Its first commercial application was as a drying agent and it is still commonly used. Sometime later, Linde synthesized zeolites X and Y; these zeolites had the structure of the natural zeolite faujasite and were also composed of sodalite cages arranged such that a 12-MR pore structure existed. The major difference between X and Y are their SiO_2/Al_2O_3 ratios in their framework. For X, this was 2–3; for Y, it was 3.5–5.5, which conferred greater hydrothermal stability, which was important in applying it to catalytic cracking.

It was then found that organic "templates" could be used to make new zeolite structures. This approach was pioneered by Mobil and led to ZK-5 (from Dabco), Beta (from tetraethylammonium ion), and ZSM-5 (from tetrapropylammonum ion), among others. Like natural zeolites, synthetic zeolites are generally named by their inventors. Since it was mostly companies that were involved in early zeolite synthesis, most names derived from them: ZSM for Zeolite Socony Mobil, LZ for Linde Zeolite, ECR for Exxon Corporate Research, and SSZ for Standard Selective Zeolite (from Chevron). This practice has continued into the present, nowadays with designations based on universities as well (for example, ITQ for Intstito de Technologia Quimica in Valencia). The International Zeolite Association has also developed a "Structure Code," which is applied to particular structure types but does not indicate chemical composition. Thus, for example, zeolite A, X and Y, and ZSM-5 are known as LTA, FAU, and MFI (for Linde Type A, Faujasite, and Mobil Five) respectively. Proposals for structure codes are made by those determining the structure and are approved by the IZA.

These three zeolites are probably the most important in terms of commercial development of zeolites. Their structures are illustrated in Fig. 0.1. The vertices in the structures represent the T atoms (Si or Al) and the lines between vertices represent the O atom bridges. This is a conventional way to represent zeolite structures, since showing all the oxygen atoms only produces a confused representation.

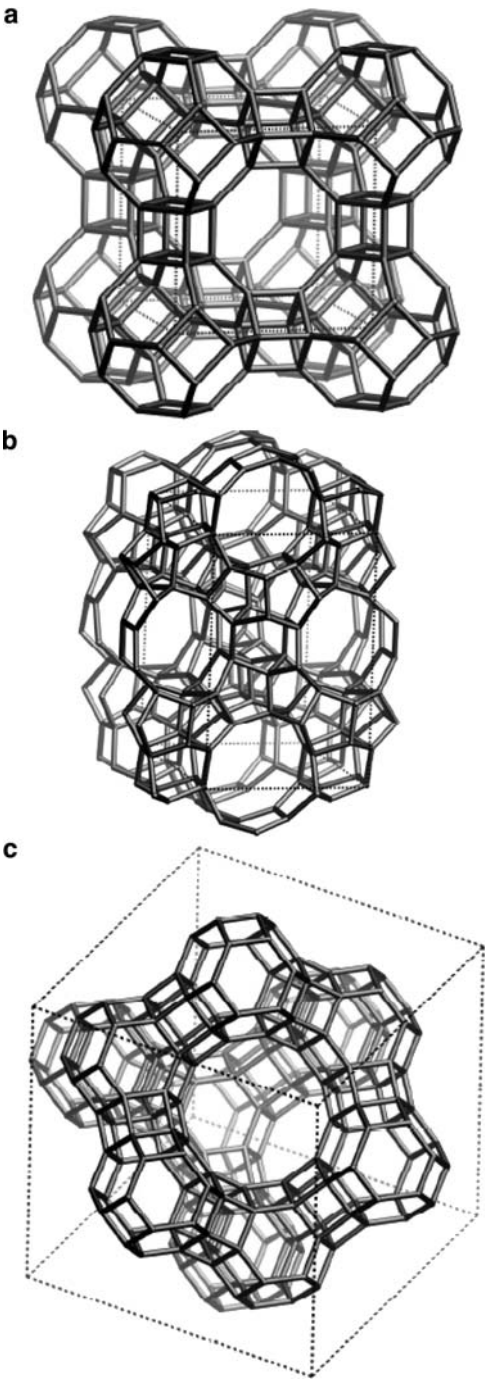

Fig. 0.1 The structures of (**a**) zeolite A (LTA), (**b**) ZSM-5 (MFI), and (**c**) faujasite (FAU). Vertices represent T atoms (Si or Al); *lines* between vertices are the O bridges. Structures taken from Baerlocher Ch, Meier WM, Olson DH (ed) (2001), Atlas of zeolite framework types, 5th edn, Elsevier, Amsterdam

Zeolite A is constructed from sodalite cages connected by 4-MR, leading to a cubic structure and three orthogonal 8-MR pores with a diameter of 4.1 Å – large enough for only small molecules, bimolecular gases, water and *n*-paraffins. Zeolite A is usually made with a SiO_2/Al_2O_3 ratio of 2, indicating equal numbers of Si and Al atoms, although different versions have been made with higher ratios. Zeolite A is generally used in adsorption and separation applications.

Faujasite (also zeolites X or Y) is also constructed from sodalite cages, but connected through 6-MR, leading to a crystallographically cubic structure in which the sodalite cages are tetrahedrally arrayed and resulting in three large orthogonal pores of 7.4 Å diameter. Most organic molecules, with some exceptions, fit into these pores. Zeolite Y has a SiO_2/Al_2O_3 ratio of 4–6 and is used in a very large scale catalytic cracking applications.

ZSM-5, on the other hand, is based on cages made of 4-, 5-, and 6-MR resulting in two elliptical pores of 5.1×5.5 and 5.3×5.6 Å normal to each other. Small and intermediate organic molecules can be adsorbed, but not larger molecules. ZSM-5 has a much higher SiO_2/Al_2O_3 ratio than the other zeolites mentioned, anywhere from around 20 to almost infinity. It is most useful in conversion of small olefins and alcohols (particularly methanol) to gasoline range hydrocarbons, as well as in shape selective cracking applications such as dewaxing.

There were 176 known structures as of 2007. An excellent source of information in general on zeolites is the Web page of the IZA (http://www.iza-online.org/). Detailed information on the structures of all known zeolite structure types is available, plus information on catalysis, synthesis, and other aspects of zeolite science.

The definition of zeolites has undergone some changes over time. Zeolites were thought to be inherently aluminosilicates, since all known examples had that composition. In the 1970s, however, Union Carbide synthesized porous zeolite-like aluminum phosphates with structures identical in some instances to known zeolites as well as new structures ($AlPO_4$s). Materials with silicon and other metals substituted for Al or P were also made that had acidity and catalytic activity (SAPOs and MAPOs). Because they were not aluminosilicates, carbide claimed that they were nonzeolitic molecular sieves (NZMSs) as a way get stronger patent claims. Similarly, carbide was able to synthesize a form of ZSM-5 that they claimed had no Al and was therefore a silicate and not a zeolite (silicalite). In fact, these latter materials had Al from the silica sources used and had SiO_2/Al_2O_3 ratios as low as 200. Nowadays, with the commercial interests out of the picture, all of these materials are recognized as part of zeolite science (in point of fact, carbide always published papers on $AlPO_4$s, SAPOs, and silicalites in the journal *Zeolites*).

Zeolites are useful in catalysis because of their acidity. Acidity arises from the Si-OH-Al grouping formed by ion exchange with acid or, more typically, by thermal decomposition of exchanged ammonium ions to form the acid group and gaseous ammonia. Zeolitic acidity is much stronger than that formed in amorphous aluminosilicates, which is usually based on the Al-OH group. Aspects of zeolite acidity are explored in detail in Chap. 3.

The most important use of zeolites, particularly by volume, is in catalytic cracking, in which the faujasite zeolites X and Y were applied by Mobil Oil in early 1960s. Prior to this, catalysts were amorphous aluminosilicates prepared by coprecipitation or cogelation, or were made from acidified natural clays. Catalytic cracking is a cyclic process in which the catalyst generates coke during the reaction and must be regenerated before reuse. Early units used swing reactors that were alternately on reaction and then on regeneration, but the more efficient cyclic units, both moving bed and fluid bed (FCC) were developed during the Second World War.

The principles of cyclic catalytic cracking are shown schematically in Fig. 0.2. Starting at the bottom of the figure and going counter-clockwise:

- Gas oil feed and regenerated (hot) catalysts are mixed and the vapor–solid mixture is transported into a reaction zone. Reaction occurs at a temperature set by the regenerated catalyst temperature and the feed initial temperature.
- Reaction products (shown to the right) are separated and sent to a downstream processing plant; spent (coked) catalyst is sent through a steam stripper into a regenerator.
- The coke on the catalyst, which contains C, H, N, and S deposited from the feed, is oxidized, heating the catalyst and releasing the gaseous compounds shown, including steam, which permanently deactivates the catalyst by dealuminization. The heated catalyst is then combined with feed and the cycle begins again.
- Fresh catalyst is added continuously or batch wise in the regenerator in order to maintain catalyst activity.

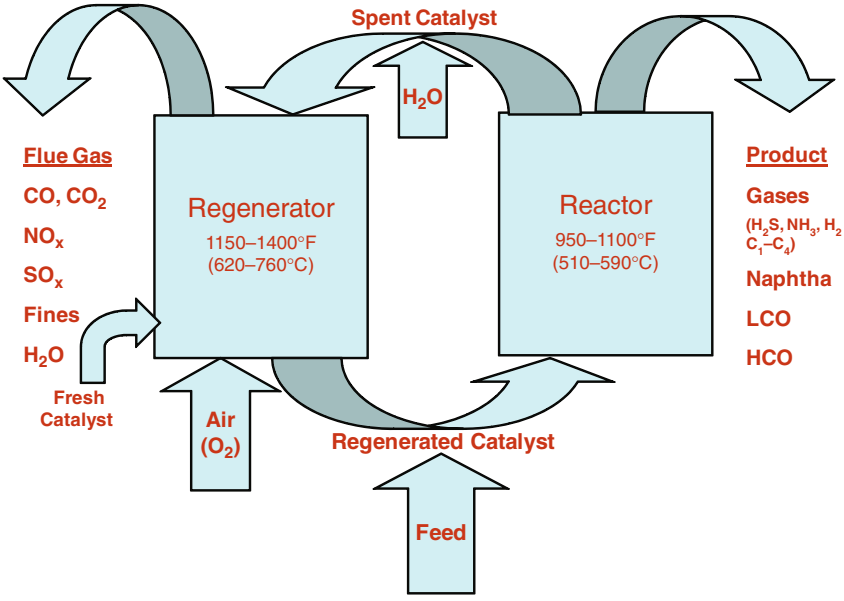

Fig. 0.2 Schematic of a cyclic catalytic cracking unit

Early proposed cracking catalysts were prepared from the low SiO_2/Al_2O_3 zeolite X, but were hydrothermally unstable. Mobil researchers discovered that exchanging zeolite X (and later zeolite Y) with mixed rare earth ions led to higher hydrothermal stability and activity (REX and REY). Early demonstrations indicated significantly higher conversions, higher gasoline selectivities, and lower coke yields than obtained with amorphous catalysts, even though early zeolite cracking catalysts contained only 5% zeolite! Although zeolite cracking catalysts did give lower octane gasoline, this could be corrected by using higher reaction temperatures, and, within 10 years of the first demonstration, zeolites were adopted throughout the industry, with REY the dominant zeolite component at up to 25–30% of the total composition, the remainder being a matrix formulated for low activity but high binder strength and low attrition. In the late 1970s, a new component USY (for ultrastable Y) began to be used to improve octane, although it had poorer hydrothermal stability. USY is a framework dealuminized version of Y made by decomposition of the $NaNH_4$ form of Y in the presence of steam at controlled temperatures. Modern catalysts generally contain rare earth-modified USY and also contain additive components for oxidizing CO to CO2 in the regenerator, reducing S and N oxides in the flue gas and for passivating metal contaminants found in the feed (particularly resids).

The success of zeolites in catalytic cracking (including hydrocracking, jointly developed by Union Carbide and Union Oil), led to significant programs at Mobil, Union Carbide, Exxon, BP, and ICI to synthesize new zeolites with improved properties. The most significant early success, as mentioned above, was the high silica zeolite ZSM-5, which was found to have revolutionary applicability in a wide number of applications: catalytic dewaxing, improving gasoline octane in FCC, conversion of methanol to gasoline (MTG) or olefins (MTO), olefin oligomerization, xylene isomerization, ethylbenzene synthesis, toluene disproportionation, and selective toluene disproportionation (directly to *p*-xylene), to name the most prominent. All of the named processes – and others – have been commercialized over different forms of ZSM-5. It is currently used in FCC to generate high volumes of propylene – an offshoot of its octane enhancement properties.

New applications continue to be discovered for existing and new zeolites. Newer materials being developed – like MOFs and mesoporous materials – may have similar successes in the future. The zeolite science taught in this volume should be of help and guide for such successes.

Cherry Hill,
NJ, USA

Arthur W. Chester
April, 2009

In Memory of Our Friend and Colleague Eric G. Derouane, 1944–2008

Eric Derouane in Paris during the 14th International Congress in Catalysis (ICC) in July 2004

Fernando Ramôa Ribeiro, Instituto Superior Tecnico, Universidade Técnica de Lisboa, Palácio Centeno, Alameda de Santo António dos Capuchos, n°1, 1169-047 Lisboa, Portugal (ramoa.ribeiro@ist.utl.pt).

Jacques C. Védrine, Laboratoire de Réactivité de Surface, Université Pierre et Marie Curie, 4 Place Jussieu, Paris, 75252, France (jacques.vedrine@upmc.fr).

And his colleagues and friends from Namur, Belgium, from Caen, Montpellier, Mulhouse, Paris, France, from Aveiro, Faro, Lisboa, Porto, Portugal, from Moskva, Russia and from Liverpool, United Kingdom.

Professor Eric Derouane died on 17th March 2008 from a heart attack in his home in Luz, Lagos, Portugal. With him, the Catalysis Community has lost one of its strongest and most brilliant scientists.

Born on 4th July 1944 at Péruwelz (Hainaut), Belgium, Eric Derouane obtained a Licence degree at the University of Liège, B (1965), a Master of Arts (MA) degree in Chemistry in Prof. J. Turkevich's laboratory at Princeton University, USA (1966) and a Doctorat ès Sciences (>PhD) at the University of Liège, B (1968), including a

year (1966–1967) in France at the "Service de Physique du Solide et de Résonance Magnétique, CEN Saclay" in Prof. A. Abragam's laboratory. He stayed a year (1969–1970) in USA at Stanford University as a visiting Scholar in Prof. M. Boudart's laboratory. He became Research Assistant of the "Fonds National de la Recherche Scientifique" (FNRS) and Lecturer at the University of Liège, B (1969–1973). In 1973, he was appointed Professor at the "Facultés Universitaires Notre-Dame de la Paix" (FUNDP) in Namur, B, where he created the Laboratory of Catalysis, of which he remained Director until 1995. He was on sabbatical in 1979 as Research Fellow with J. Sinfelt at Exxon Res. & Develop. Corp., Linden, USA, and in 1982–1984 as Research Scientist, Head of Exploratory Catalysis Synthesis Group at Mobil Res. & Develop. Corp., Central Research Laboratory, at Princeton, USA.

In 1995, he became Full Professor at the University of Liverpool and was appointed Director of the Leverhulme Centre for Innovative Catalysis (LCIC).

In 2003, he obtained the prestigious Gulbenkian Professorship at the University of Algarve in Faro, P, where he was the Director of the Chemical Research Centre. Later, he also became invited Professor at the "Instituto Superior Tecnico" (IST) of the Technical University of Lisbon, where he had extensive cooperation with the group led by Prof. F. Ramôa Ribeiro.

His main fields of investigation dealt with catalysis over zeolites in general, supported metals, novel materials and mixed oxides in particular, and alkane upgrading and fine chemicals more specifically. One of Eric's most striking qualities was his acute interest for every new scientific discovery and for industrial applications of his findings.

Eric worked with unusual efficiency. He had a high intellectual mobility and was always attracted by new materials and new concepts. Among them, one can mention the new zeolite ZSM-5/MFI in the early 70s, leading to 30 year collaboration with J.C. Védrine; cuprate-type superconductors and confinement effects and molecular traffic control in microporous zeolitic materials. He also studied reaction mechanisms using isotopic labelling and in situ MAS-NMR in the 80s, combinatorial catalysis and high throughput technology in the late 90s.

During his 20 years of dedicated service to the University of Namur, Eric developed new concepts, which had an important impact on catalysis and zeolite communities. In 1986, he was elected Head of the Chemistry Department. He then embarked upon an impressive re-structuring program to improve its efficiency. The model which he initiated is still in service today. His laboratory was recognized as an outstanding school of scientific research and education in catalysis.

Quite early on, Eric realized the importance of interdisciplinarity, which led him to play a key role in the creation of the Institute for Studies in Interface Sciences (ISIS) at Namur in 1987, which incorporated laboratories of physics and chemistry for 20 years. Eric Derouane also paid heed to technology transfer to industry. After his experience gained through his sabbatical positions at Exxon and Mobil, he developed collaborations with industrial partners and served as consultant for many companies.

At Liverpool, the aim of the LCIC was to promote creative fundamental catalytic science and often to take-up industrial challenges. Eric defined innovation as "the creation of new or better products or processes, implying creativity, usefulness, and application." Towards this end, the LCIC had industrial affiliates as partners. Under his leadership, the LCIC became the largest catalysis centre in the UK and a centre of scientific exchanges and collaborations. Eric established links with many UK and international laboratories. He created in 1997 an European Associated Laboratory "Laboratory for high specificity catalysis" between LCIC/University of Liverpool and Institut de Recherches sur la Catalyse, Lyon / CNRS, of which J.C. Védrine became the Director in 2003.

In 1999, he co-founded with Prof. S. Roberts the *spin-off* Liverpool-based company "Stylacats," of which he became the Director. He provided wise suggestions and ideas, which led the company to pioneer new technologies, particularly catalysts for asymmetric hydrogenation, microwave-induced reactions and enzyme mimetics.

At the University of Faro, Eric developed a research project jointly with the Instituto Tecnico de Lisboa on Friedel-Crafts reactions. He also collaborated closely on various research projects with Prof. F. Ramôa Ribeiro's zeolite group of the Instituto Superior Tecnico of the Technical University of Lisbon.

Eric co-authored over 400 scientific papers, 11 books and 61 patents.

Eric Derouane has contributed greatly to the development and strengthening of the European Catalysis Community. He created in 1975 the European Association in Catalysis (EUROCAT), a consortium of more than 30 European laboratories under the auspices of the Council of Europe and promoted standardisation of characterisation of catalysts: For this purpose, catalysts such as Euro-Pt1 to -Pt4 (Pt/SiO_2 and $Pt\text{-}Re/SiO_2$), Euro-Ni1 & -Ni2 (Ni/SiO_2), Eurocat zeolite (TS1-type), Eurocat oxides (V_2O_5/TiO_2 and $V_2O_5\text{-}WO_3/TiO_2$) were synthesized by industrial companies (Johnson Matthey from United Kingdom, Unilever from the Netherlands, Rhône Poulenc from France, industrial partner from Austria) and distributed to the 30 laboratories in Europe for characterisation. This work led to several articles by G. Bond, J. Coenen, P. Wells and others in Applied Catalysis in the '80s or several special issues of Catalysis Today by J.C. Védrine and others in the '90s to help any scientist to calibrate his/her characterisation techniques by having standard and well-characterized samples.

This Eurocat group paved the way for the creation of the European Federation of Catalysis Societies (EFCATS) and of the François Gault lectureship for which Eric played a decisive role. He was elected President of EFCATS in 1995 for 2 years.

Eric Derouane was the Editor-in-chief of J. Mol. Catal.A: Chemical from 1982 till his death. He was the member of the Editorial Boards of many scientific journals and member of the scientific committees of many congresses and colloquia. He co-organized several congresses himself, particularly with Prof. F. Lemos and F. Ramôa Ribeiro in Portugal on several NATO Advanced Studies Institutes on topics including "the conversion of light alkanes," "combinatorial catalysis and high throughput catalyst design and testing," "principles and methods for accelerated catalyst design and testing" and "sustainable strategies for the

upgrading of natural gas." The content of these summer schools was published in NATO editions by Riedel & Co.

Eric's contributions to catalysis have been recognized by many awards and academic honors, including the Wauters Prize (1964), the Mund Prize (1967) of the "Société Royale de Chimie," the Stas-Spring Prize (1971) and the Adolphe Wetrems Prize (1975) of the "Académie Royale de Belgique," the Rosetta Briegel-Barton Lecturership at the University of Oklahoma (1973), the Prize of the "Cercle of Alumni de la Fondation Universitaire de Belgique" (1980), the Ciapetta Lectureship of the North American Catalysis Society (1981), the Catalysis Lectureship of the Société Chimique de France (1993) and the prestigious Francqui Prize, B (1994), the highest honor for all Sciences in Belgium.

He was made "Officier de l'Ordre Léopold" in Belgium (1990), corresponding Member of the "Académie Royale des Sciences, des Lettres et des Beaux Arts de Belgique" (1991), member of the "New York Academy of Sciences" and Associate Member of the "European Academy of Arts, Sciences and Humanities." He was conferred Doctor Honoris Causa by the Technical University of Lisbon (1996).

Eric attracted many students and scholars to his laboratories in Namur, Liverpool and Faro. His energy, clear mind and broad knowledge impressed his students, researchers and colleagues. He was an outstanding and demanding professor, always ready to share his knowledge with his students. His courses were always clear, highly structured and easily understandable. Many of his former students and post-docs occupy today prominent positions in universities and industries. All of them will remember his brilliant and rigorous scientific approach and no doubt, will greatly miss him.

In honour of him, many of Eric's friends and colleagues decided to pay their tribute to him by participating to a two days symposium organized in Lisbon at the Instituto Superior Tecnico of the Technical University of Lisbon on 25–26 September 2008 and organized by Prof. Jacques C. Védrine and by Prof. Fernando Ramôa Ribeiro and his team. Almost one hundred participants attended this symposium from all over the world, in particular from Belgium, Canada, Denmark, France, Italy, Poland, Portugal, Russia, South Africa, Spain, United Kingdom, etc. Many messages of sympathy were received from all over the world as recognition of his worldwide influence. The scientific contributions for this symposium were in all his fields of interest with particular emphases to zeolites, confinement effect, molecular traffic control and catalytic reaction mechanism using MAS-NMR technique, both in heterogeneous and homogeneous catalysis and both from industrial and academic scientists, in excellent coherence with his own scientific career. A special issue of his journal: "*Journal of Molecular Catalysis A: Chemical*" will assemble all contributions and will appear by mid-2009.

Contents

Contributors

Aline Auroux
Institut de Recherches sur la Catalyse et l'Environnement de Lyon, UMR 5256 CNRS/Université Lyon1, 2 avenue Albert Einstein, 69626 Villeurbanne Cedex, France, aline.auroux@ircelyon.univ-lyon1.fr

Allen W. Burton
Chevron Energy Technology Company, 100 Chevron Way, Building 50, Office 1254, Richmond, CA 94802, USA, buaw@chevron.com

Ljiljana Damjanović
Institut de Recherches sur la Catalyse et l'Environnement de Lyon, UMR 5256 CNRS/Université Lyon1, 2 avenue Albert Einstein, 69626 Villeurbanne Cedex, France
Faculty of Physical Chemistry, University of Belgrade, Studentski trg 12-16, 11000 Belgrade, Serbia

Matteo Guidotti
CNR-Istituto di Scienze e Tecnologie Molecolari, IDECAT-CNR Unit, Dip. Chimica IMA "L. Malatesta", via G. Venezian, 2120133 Milano, Italy, m.guidotti@istm.cnr.it

Michel Guisnet
UMR CNRS 6503, Université de Poitiers (France), Departamento de Engenharia Quimica, IST-Technical University of Lisbon, Av. Rovisco Pais, 11049-001 Lisboa, Portugal, michel.guisnet@univ-poitiers.fr

Michael Hunger
Institute of Chemical Technology, University of Stuttgart, 70550 Stuttgart, Germany, michael.hunger@itc.uni-stuttgart.de

Christine E. Kliewer
ExxonMobil Research & Engineering, 1545 Route 22 East, Annandale, NJ, 08801, USA, chris.e.kliewer@exxonmobil.com

Xinsheng Liu
BASF Catalysis Research, R&D Center, 25 Middlesex-Essex Turnpike, Iselin, NJ 08830, USA, xinsheng.liu@basf.com

Evgeny A. Pidko
Schuit Institute of Catalysis, Eindhoven University of Technology, 513, NL-5600 MB Eindhoven, The Netherlands, e.a.pidko@tue.nl

Rutger A.van Santen
Schuit Institute of Catalysis, Eindhoven University of Technology, 513, NL-5600 MB Eindhoven, The Netherlands

Michael Stöcker
SINTEF Materials and Chemistry, 124 Blindern, 0314, Oslo, Norway, michael.stocker@sintef.no

Chapter 1
Powder Diffraction in Zeolite Science

An Introductory Guide

Allen W. Burton

Abstract This tutorial discusses the fundamental principles of X-ray diffraction and its applications in zeolite science. The early sections review the physics of diffraction, crystal symmetry, and reciprocal space. We discuss how the intensity of diffracted radiation is affected both by geometric effects involving detection (the Lorentz-polarization factor) and by the arrangement of atoms within the crystal (the structure factor). The differences between powder diffraction and single-crystal diffraction are then described, and differences between X-ray and neutron diffraction are also discussed. Later sections describe the effects of symmetry, lattice substitution, crystallite size, residual strain, preferred orientation, and X-ray absorption. Special emphasis is placed on the proper application of the Scherrer analysis in reporting crystalize size. The principles of structure solution from direct methods and Patterson methods are then introduced, and a description of Rietveld analysis is given. Finally the effects of stacking disorder on a powder diffraction pattern are presented.

1.1 Introduction

X-ray diffraction (XRD) is an essential tool in the identification and characterization of zeolites at various stages in their syntheses, modifications, and uses as catalysts. Because the typical student is expected to use several characterization methods in his studies of zeolites, attaining a thorough understanding of powder diffraction can initially be daunting for the investigator who wishes to use XRD as more than a "fingerprint" for phase identification. A detailed molecular understanding

A.W. Burton
Chevron Energy Technology Company, 100 Chevron Way, Building 50, Office 1254, Richmond, CA 94802, USA
e-mail: buaw@chevron.com

A.W. Chester and E.G. Derouane (eds.), *Zeolite Characterization and Catalysis*,
DOI 10.1007/978-1-4020-9678-5_1,

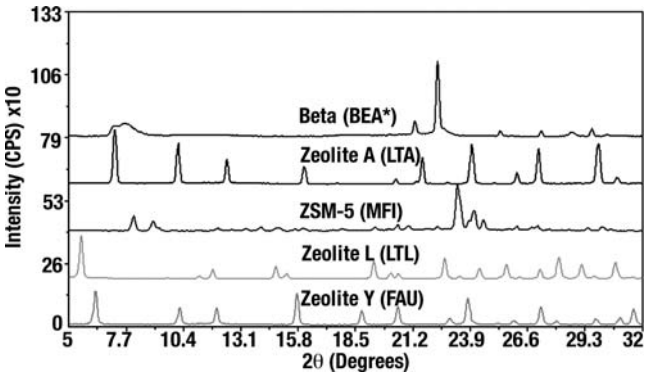

Fig. 1.1 Powder XRD patterns of selected zeolites with important commercial applications

of zeolite structures is essential in explaining their catalytic, adsorption, and ion-exchange properties. XRD allows us to examine the long-range atomic structure of crystalline materials. For zeolites this includes the framework topology and the positions of extra-framework cations and/or adsorbed molecules. Cations strongly influence adsorption and catalysis in zeolites through the interactions they have with guest species.

Figure 1.1 shows powder XRD patterns for five zeolites that have important commercial applications. Note that the patterns of each zeolite are very distinct from one another. Much information may be gleaned from a powder diffraction pattern: the topological and long-range structure of a material, the approximate crystal size of the material, strain or stress in the material, the approximate extent of heteroatom substitution, crystallinity, or the presence of stacking disorder. This chapter begins by discussing fundamental concepts of crystal symmetry, diffraction, reciprocal space, and scattering. Differences between single crystal diffraction and powder diffraction will then be discussed. We will then describe how crystallite size, strain, absorption, preferred orientation, and instrumental broadening affect a powder pattern. Next we will briefly describe methods used to solve and refine crystal structures. Finally, the qualitative effects of stacking disorder will be discussed.

Throughout this chapter, theory is provided to enhance the reader's understanding, but many practical examples are also given to illustrate important concepts. For the beginning student, I highly recommend the practical guides by Bish and Post [1], Jenkins and Snyder [2], and Chung and Smith [3]. The books by Cullity [4], Warren [5], Klug and Alexander [6], and Giacovazzo [7] provide excellent combinations of instructive theory and applications. Warren [5] and Guinier [8] provide thorough mathematical treatments of diffraction, and they give excellent discussion on the effects of disorder in crystalline materials. For explanations of methods involved in crystal structure determination, I recommend the book by Stout and Jensen [9] and the monograph by David et al. [10]

1.2 Lattice Spacings, Unit Cells, Crystal Symmetry, and Space Groups

It is instructive to clarify terms that are often used in the discussion of crystal structures (the book by Burns and Glazer provides useful discussion [11]). A *lattice* is an infinite array of points in space in which each point has identical surroundings to the others. In the case of a crystal structure, the surroundings of each lattice point are defined by the periodic arrangement of atoms in space. Each lattice point can be related to another by an integral number of translations in the *a*, *b*, and *c* directions. The vectors *a*, *b*, and *c* enclose a volume known as the *primitive unit cell*. Primitive unit cells contain only one lattice point, but it is sometimes more convenient to use unit cells with multiple lattice points. For example, a body-centered (i.e., a unit cell with a lattice point also at 1/2*a*, 1/2*b*, 1/2*c* if the origin is chosen as a lattice point) unit cell possesses two lattice points. The *unit cell parameters* define the magnitudes of the unit cell vectors and the angles between them.

The crystal structure is described by associating each lattice point with a group of atoms within the unit cell known as the *basis*. The basis includes the atoms and their positions. From the basis, the unit cell composition can be directly determined and is often listed, for example, in the Atlas of Zeolite Framework Types [12] or in the Collection of Simulated XRD Patterns for Zeolites [13]. The *space group* is the set of symmetry operations that take a three-dimensional periodic object into itself. The *asymmetric* unit is the smallest region of space that fills all space when these symmetry operations are applied. If the atoms within the asymmetric unit are specified, then the basis of atoms in the unit cell is produced by the symmetry operations of the space group. In a typical crystallographic report, the asymmetric unit, unit cell parameters, and space group are provided. These can be used as input to software such as Cerius [14] or ORTEP [15] to provide three-dimensional views of the structure with as many unit cells in the three dimensions that the investigator wishes to visualize. In the patent literature, inventors of new materials occasionally list the coordinates for the entire basis of atoms in the unit cell of the crystal structure. The space group symmetry and unit cell parameters of the material are sometimes not provided in the patent, but in some cases they can be inferred.

Each space group symbol provides enough information to determine all the symmetry operations performed by the space group. For example, the structure of ITQ-3 (ITE) has the orthorhombic space group symmetry *Cmcm*. The "*C*" indicates the unit cell is face-centered on the *a*–*b* plane at $c = 0$ (i.e., there is a lattice point at 0,0,0 and 1/2, 1/2, 0). The first "*m*" indicates there is a mirror plane perpendicular to the *a*-axis, the "*c*" indicates there is a glide plane perpendicular to the *b*-axis, and the second "*m*" indicates there is a mirror plane perpendicular to the *c*-axis. A glide plane is an operation in which a reflection across a plane is followed by a translation; in the current example, the "*c*" glide plane indicates a reflection across a plane perpendicular to b followed by a translation 1/2*c*. Other glide planes include the "*n*" and "*d*" glide planes. In an *n*-glide plane that is perpendicular to the *c*-axis, the reflection across the plane is followed by translations of 1/2*a* and 1/2*b*.

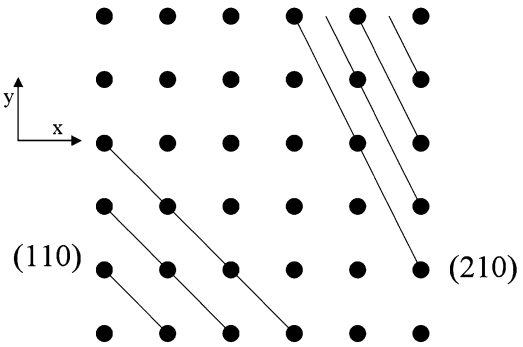

Fig.1.2 Illustration of the (*110*) and (*210*) Miller plane. The *z*-direction is perpendicular to the plane of the paper

For higher symmetry (hexagonal, tetragonal, cubic) lattices in which the *a*- and *b*-axes are symmetry-equivalent, the order of the space group symbols carries different meaning with regard to the positions of symmetry axes or planes. For example, let us consider the cubic space group *I432*. In this body-centered space group, there are four-fold rotation axes along the *x*-, *y*-, and *z*-axes. There are threefold rotation axes along the diagonals of the unit cell and twofold rotation axes along the diagonals of each face of the unit cell. The twofold rotation axes do not help to define the space group since they can be derived from the other symmetry operations.

The lattice points of a given crystal structure define an infinite number of families of parallel planes. Each family of parallel planes in the lattice is defined by the set of Miller indices *h k l*. The lattice points repeat in the *x*, *y*, and *z* (not necessarily perpendicular) directions with distances of *a*, *b*, and *c* respectively. If one lattice point is chosen as the origin, then the intercepts of all planes (along the *x*, *y*, and *z* axes) can be expressed as *ma*, *nb*, and *pc* where *m*, *n*, and *p* are integers or infinity. In terms of the Miller indices

$$h \propto \frac{1}{m}\,,\; k \propto \frac{1}{n},\; l \propto \frac{1}{p}$$

so $h = np/t$, $k = mp/t$, and $l = mn/t$, where t is the greatest common divisor of np, mp, and mn. Figure 1.2 shows examples of the (210) and (110) planes for a lattice in which a and b are equal (but not necessarily identically equal).

1.3 Fundamentals of Diffraction and Reciprocal Space

Figure 1.3 shows two infinite parallel planes separated by a distance d. If monochromatic radiation (for diffraction this will typically be X-rays, neutrons, or electrons) of wavelength λ strikes those planes at an angle θ, constructive interference will occur when the path difference between the diffracted (or reflected) waves

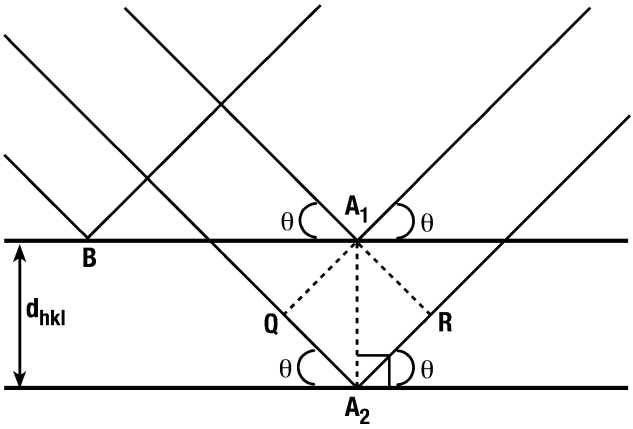

Fig.1.3 Illustration of diffraction from two parallel planes. Constructive interference occurs when the path difference (i.e., $QA_2 + A_2R = 2d_{hkl}\sin\theta$) of the reflected waves is equal to an integral number of wavelengths. Figure adapted from [2]

from each plane is equal to an integral number, n, of wavelengths. The rays in Fig. 1.3 are shown such that the distance A_1A_2 is equal to the distance between the parallel planes. It is straightforward to show that constructive interference occurs when

$$n\lambda = 2d\sin\theta \tag{1.1}$$

This condition applies regardless of where the parallel rays strike the planes. For example, parallel rays that strike the first plane at points B and A_1 will both be in phase with the rays that reflect from the second plane when the Bragg equation is satisfied. Can you prove this? Note that the lower limit for a detectable "d" spacing is $\lambda/2$ since $\sin\theta \leq 1$. This explains why X-rays are suitable for diffraction studies of crystalline materials. For visible light ($\lambda \sim 5{,}500$ Å), the lowest detectable d-spacing is about 2,750 Å. This is clearly larger than the unit cell dimensions of most crystalline materials (zeolite cell dimensions are typically found in the range of 5–80 Å).

It can be shown that the distance, d_{hkl}, between a set of hkl planes in an orthorhombic lattice (a lattice where symmetry constraints force the x, y, and z directions to be mutually perpendicular, but the dimensions are not identically equal) can be determined from the relation

$$\frac{1}{{d_{hkl}}^2} = \frac{h^2}{a^2} + \frac{k^2}{b^2} + \frac{l^2}{c^2}$$

Similar equations may be derived for other lattice systems. Hence, from the measured positions of diffraction peaks, information on the unit cell parameters can be determined.

1.3.1 Ewald Sphere of Reflection and Reciprocal Space

In some discussion of diffraction, it is more convenient to use the "reciprocal space lattice" rather than the real space lattice. The reciprocal lattice is more applicable to the interpretation of diffraction data because, in essence, the diffraction pattern is a manifestation of the reciprocal lattice. We can define a space of vectors of magnitude $1/d_{hkl}$ (i.e., the "reciprocal" of the d-spacing) that are perpendicular to their respective *hkl* plane. Each *hkl* reciprocal space vector is expressed as $\mathbf{r}^* = h\mathbf{a}^* + k\mathbf{b}^* + l\mathbf{c}^*$. The reciprocal lattice spacing $\mathbf{a}^*$ is defined such that $\mathbf{a}^* \cdot a = 1$ and $\mathbf{a}^* \cdot b = \mathbf{a}^* \cdot c = 0$ (i.e., the reciprocal lattice vector $\mathbf{a}^*$ is perpendicular to the real space vectors **b** and **c**). Analogus expressions apply to $\mathbf{b}^*$ and $\mathbf{c}^*$. Note that each of the reciprocal space lattice vectors is parallel to the real space lattice vector in lattices with orthogonal cell parameters.

The reciprocal lattice can be used to understand Bragg's law in a pictorial fashion using the concepts of the Ewald (or reflection) sphere and the limiting sphere. In Fig. 1.4 we have drawn two spheres that are tangent to one another at point Q: the Ewald sphere has radius $1/\lambda$ and the limiting sphere has radius $2/\lambda$. Point *P* is the center of the smaller sphere and corresponds to the position of our crystal. The center of the larger circle is at point O, which is where we will assign the origin of the reciprocal lattice. When diffraction occurs, the angle between the primary beam along QP and the diffracted beam along PR is 2θ. The intersection of

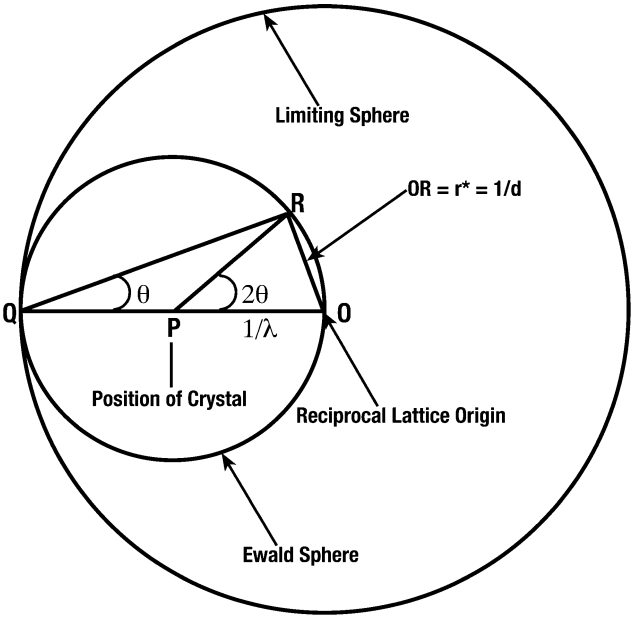

Fig. 1.4 Illustration of Ewald sphere and the limiting sphere of reflection. The images on the next page show points of the reciprocal lattice as it rotates

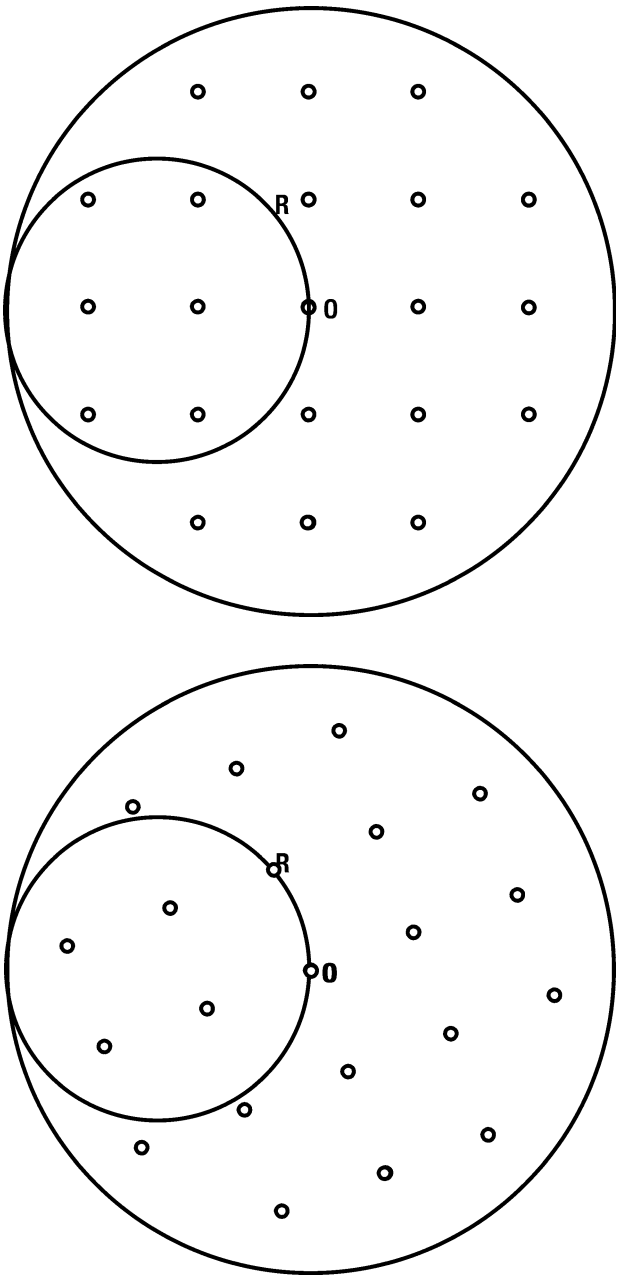

Fig. 1.4 (Continued)

the diffracted beam with the Ewald sphere occurs at point R. The angle $\angle$PQR equals θ (can you prove that?). Note that OR = OQ $\sin\theta = 2\sin\theta/\lambda$. If we state that OR = $\mathbf{r}^*$ (which is true since O is the origin of the reciprocal lattice), then the previous equation is equivalent to Bragg's law since $\mathbf{r}^* = 1/d$. Therefore, if the reciprocal lattice is rotating about point O (as the crystal is being rotated), then diffraction occurs when a reciprocal lattice point intersects the Ewald sphere. If the reciprocal lattice vector has magnitude $r^* > 2/\lambda$, then $\mathbf{r}^*$ lies outside the limiting sphere and it is impossible for its reciprocal lattice point to intersect the Ewald sphere. This is equivalent to the statement near the beginning of this section that d_{hkl} must be greater than $\lambda/2$ in order for diffraction to occur. By completely rotating the reciprocal lattice in all possible directions, all lattice spacings with $\mathbf{r}^* < 2/\lambda$ will pass through the Ewald sphere. In subsequent sections, the reciprocal lattice will be used to explain other concepts of diffraction.

1.4 Single Crystal Diffraction

It is from the *hkl* families of planes that diffraction of X-rays occurs within a given crystal. Figure 1.5 shows a single crystal diffraction pattern of zeolite RUB-3 (RTE) along the *hk0* zone. [16] This image contains the diffraction spot for each measurable *hk0* reflection. From this diffraction pattern, we are able to infer the *d*-spacings

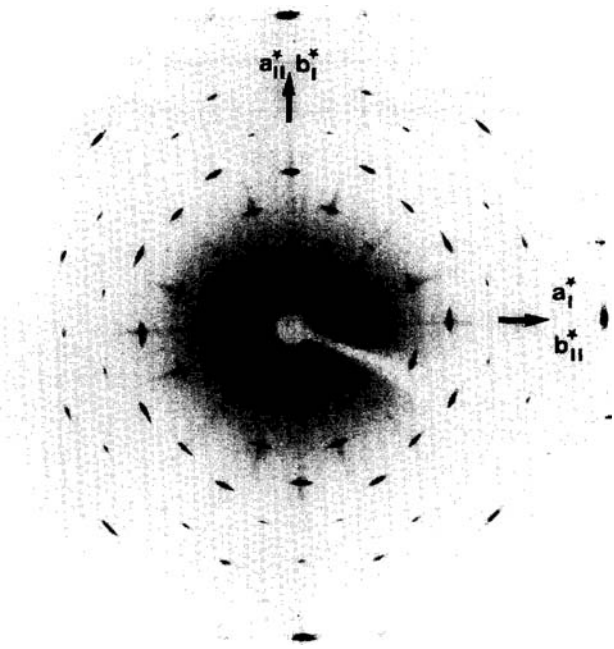

Fig.1.5 Precession photograph of the *hk0* layer of RUB-3. Reprinted from [16] with permission from Elsevier

within the *a–b* plane and therefore the likely cell dimensions along the a- and b-directions. If the film is perpendicular to the primary beam, the diffraction angle θ for each spot is equal to $\tan^{-1}(r/D)/2$, where D is the distance from the sample to film and r is the distance of the diffraction spot from the spot for the direct beam.) By rotating a crystal, we are able to record diffraction patterns along other (*hkl*) zones and thereby create a mapping of the diffracted intensity in three-dimensional space.

Many single crystal diffraction studies today are performed with four-circle diffractometers. By rotating a crystal around three axes as it is being irradiated, all measurable *hkl* planes may be placed in a position to diffract and a recording can be made for the measured intensities of each position of the detector in three-dimensional space.

1.5 Intensity From Diffraction

In order to obtain information about atomic structure from intensity data, we must first understand all the factors that contribute to the measured intensity of an *hkl* reflection. Relative peak intensities are a function not only of the atomic structure of the material, but also of angle-dependent geometric factors that result from the detection of the diffracted radiation and from the polarization of the radiation source. This section explains these factors. The integrated intensity for a given Bragg reflection is given by

$$I(hkl) = KL_p(\theta)|F(hkl)|^2 \tag{1.2}$$

K is a constant that depends on the intensity and wavelength of the incident beam, the distance from the detector to the sample, the properties of the electron (for X-ray scattering), the unit cell volume, and the total volume of the irradiated sample. $L_p(\theta)$ is the *Lorentz-polarization factor* at the diffraction angle for the *hkl* reflection, and *F(hkl)* is the *structure factor* for the *hkl* reflection.

1.5.1 The Lorentz-Polarization Factor

The Lorentz-polarization factor contains corrections which account for (1) the polarization (or lack thereof) of the radiation source and (2) geometric effects involved in the detection of the diffracted radiation (often referred to as the Lorentz component). The polarization component can be expressed generally as $K_1 + K_2\cos^2(2\theta)$. This term arises because the primary beam possesses electric field components that lie perpendicular and parallel, respectively, to the plane containing the primary beam and the scattered radiation. An electric field induces oscillatory motion in the electrons of an atom. It is this motion that gives rise to the scattered radiation. If the radiation is unpolarized, then $K_1 = K_2 = 1/2$.

For scattering of neutrons, there is no polarization of the radiation, and so the polarization term is replaced by a factor of 1. When single crystal monochromators are used, additional terms are required for the polarization correction because the monochromator partially polarizes the X-ray beam.

For a single crystal irradiated by unpolarized radiation, the entire Lorentz-polarization factor is expressed as

$$L_p = \frac{1 + \cos^2(2\,\theta)}{2\ \sin(2\theta)} \tag{1.3}$$

The factor $1/\sin(2\theta)$[1] arises because the time required for a reciprocal lattice point to pass through the Ewald sphere (i.e., to be in diffracting position) is not constant; that is, the time varies with the position of the lattice point in reciprocal space and the direction in which it approaches the Ewald sphere. As a result, the reciprocal lattice points remain within detection range for different periods of time. In my experience, I admittedly have initially found this to be a difficult concept to grasp. It is useful to visualize the Ewald sphere as a shell that has some infinitesimal thickness ΔR as shown in Fig. 1.6. In a typical single crystal experiment, the crystal is rotated around an axis perpendicular to the plane of the incident and diffracted beams at a constant angular velocity ω. The reciprocal lattice (centered at point O) therefore also rotates with this same angular velocity. Our goal is to find the amount

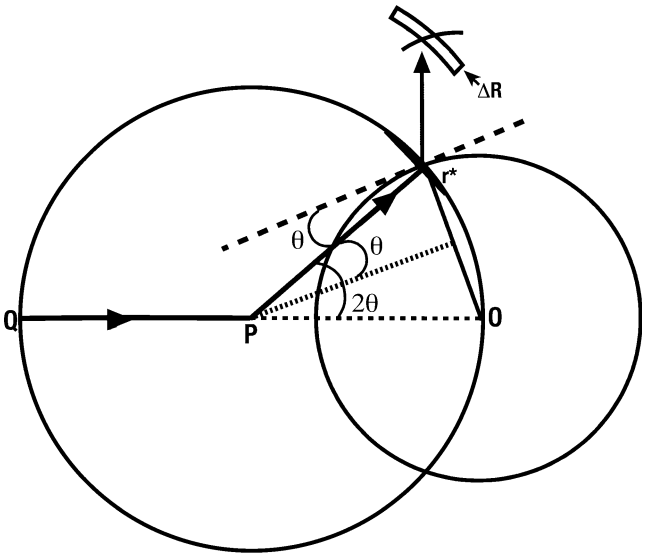

Fig.1.6 Illustration of reciprocal lattice point passing through the Ewald sphere of reflection

[1]This assumes that the axis of rotation of the crystal with respect to the incident beam is 90°.

of time that a reciprocal lattice point remains within the shell of the Ewald sphere. The linear velocity of the reciprocal lattice point is $\mathbf{r}^*\omega$. The time required for the lattice point to pass through the shell is equal to the shell thickness (ΔR) divided by the component of the linear velocity that lies along the radius of the Ewald sphere. This component of the velocity is $\mathbf{r}^*\omega\cos\theta = (2\omega\sin\theta\cos\theta)/\lambda = \omega\sin 2\theta/\lambda$. The time is therefore proportional to $1/(\sin 2\theta)$.

For a randomly oriented powder, the Lorentz-polarization factor is given by

$$L_p = \frac{1+\cos^2(2\,\theta)}{\sin(\theta)\,\sin(2\theta)} \tag{1.4}$$

In this case an additional factor of $\cos\theta/\sin(2\theta)$ has been multiplied by the single crystal factor. The additional factor has two different sources: (1) it represents the fraction of crystallites in the powder that are oriented in such a way to diffract at the Bragg angle ($\cos\theta$ term) and (2) it accounts for the fact that the intensity of each reflection at a given Bragg angle is distributed over a circular ring with a circumference that changes with the diffraction angle ($1/\sin 2\theta$). From Fig. 1.7 we can determine the origin of the $\cos\theta$ term. For a perfectly random distribution of crystallites, the normal vectors of each *hkl* plane will uniformly cover the surface of a sphere of radius *R* around the sample. When diffraction occurs from these *hkl* planes, the angle between the primary beam and their normal is $(90-\theta)$. The key then is to find the fraction of normal vectors that are at an angle $(90-\theta)$ to the primary beam. Since a given *hkl* vector uniformly covers the surface of this sphere,

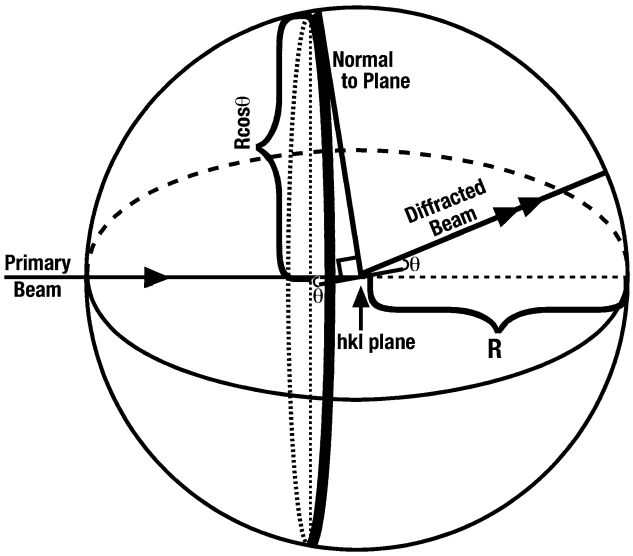

Fig.1.7 Illustration used to estimate fraction of crystallites that are in a position to diffract at a given angle θ. This fraction gives rise to the $\cos\theta$ factor in the Lorentz polarization correction

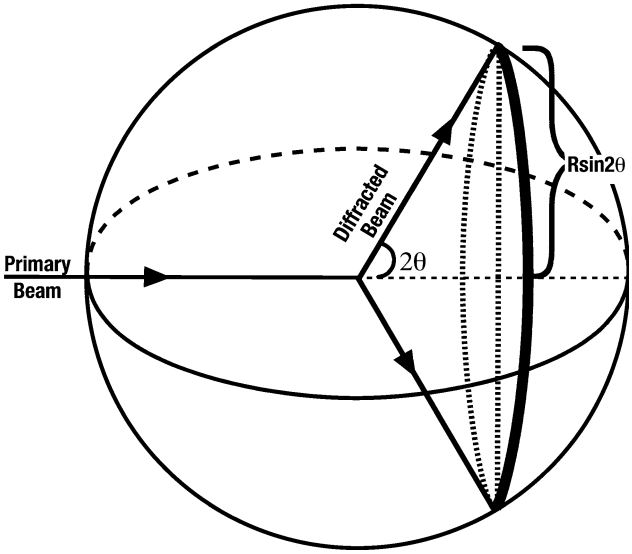

Fig.1.8 Illustration of the powder ring distribution that gives rise to the $1/\sin 2\theta$ term in the Lorentz polarization factor

this can be found by determining the area of a circular band of infinitesimal width that surrounds the sphere at an angle $(90-\theta)$. The radius of this band is $R\cos\theta$, and the area of the band is therefore proportional to $\cos\theta$.

The $1/\sin 2\theta$ term arises from the fact that the intensity of a reflection is distributed over the circle of a diffraction cone (Fig. 1.8) with radius proportional to $\sin 2\theta$, and so the intensity per unit length is proportional to $1/\sin 2\theta$. These circular bands sometimes are referred to as "Debye" rings. An analogy would be that of a circular rubber band with an even distribution of particles on its surface whose radius changes with the diffraction angle. Because the detector measures intensity only at a single point along the circle of the cone and does not measure the integrated sum of intensities around the entire circular band, the measured intensity is, in effect, diluted by a factor proportional to the circumference of the circle.

After these factors are multiplied by the single crystal factor, we obtain the entire Lorentz contribution for powder diffraction:

$$\frac{\cos\theta}{\sin 2\theta \sin 2\theta} = \frac{\cos\theta}{2\cos\theta \sin\theta \sin 2\theta} = \frac{1}{2\sin\theta \sin 2\theta}$$

Figure 1.9 shows a graph of the Lorentz-polarization factor for powder diffraction. Here it can be seen that the Lorentz-polarization correction is very large at low angles and that it reaches a minimum around 100°. This is one reason that low-angle peaks tend to be of greater intensity than high angle peaks in powder diffraction patterns. Also, when one is comparing powder patterns of the same material collected with different wavelengths, it is important to remember that the relative

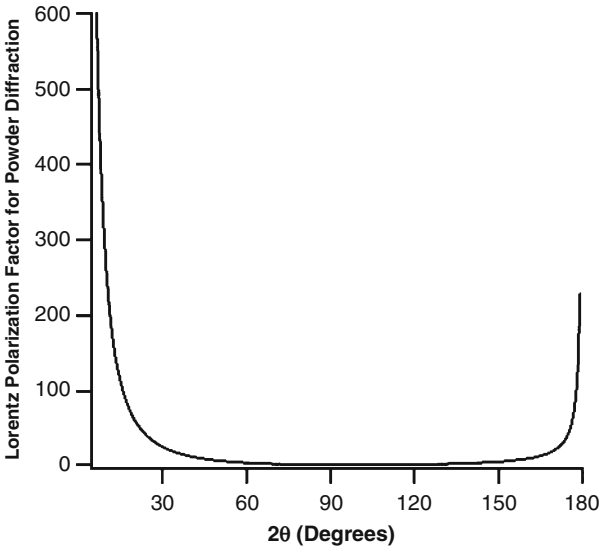

Fig. 1.9 The Lorentz polarization factor as a function of 2θ for powder diffraction

intensities of the same *hkl* peak will vary between the data sets because they possess different L_p values. This is particularly relevant for the low-angle peaks, where a change of a few degrees has significant effects on the L_p correction.

1.5.2 The Structure Factor

The structure factor for a given *hkl* reflection is given by

$$F(hkl) = \sum_j p_j f_j \exp\left(\frac{-B_j \sin^2\theta}{\lambda^2}\right) \exp\left[2\pi i\left(h x_j + k y_j + l z_j\right)\right] \qquad (1.5)$$

where the sum is over all atoms in the unit cell, f_j is the scattering factor of atom j, p_j is the fractional occupancy of atom j, and x_j, y_j, and z_j are the fractional coordinates of atom j.

The term $\exp(-B_j \sin^2\theta/\lambda^2)$ is a correction to the scattering factor that accounts for the thermal motion of the atom. The B_j term is a measure of the root-mean-square amplitude of the vibration of the atom. Care must be used in interpreting the f_j; in many references this term actually designates

$$f_j \exp\left(\frac{-B_j \sin^2\theta}{\lambda^2}\right)$$